Journal of Inorganic and General Chemistry
ZAAC
Zeitschrift für anorganische und allgemeine Chemie
www.zaac.wiley-vch.de
RESEARCH ARTICLE



DOI: 10.1002/zaac.202200265

Special Collection

# Coordination chemistry of pnictogenylboranes towards group 6 transition metal Lewis acids

Felix Lehnfeld,[a] Oliver Hegen,[a] Gábor Balázs,[a] Alexey Y. Timoshkin,[b] and Manfred Scheer*[a]

*Dedicated to Professor Sjoerd Harder on the occasion of his 60th birthday.*

The coordination behavior of different pnictogenylboranes towards group 6 metal Lewis acids is investigated. The resulting complexes with phosphanylboranes $[(CO)_4M(PH_2BH_2\cdot NMe_3)_2]$ (M=Cr, Mo, W; **1–3**), arsanylboranes ($[(CO)_4M(AsH_2BH_2\cdot NMe_3)_2]$ (M=Cr, Mo, W; **4–6**) and *t*Bu-substituted phosphanylboranes $[(CO)_4M(t\text{BuPHBH}_2\cdot NMe_3)_2]$ (M=Cr, W; **7–8**) are fully characterized by multinuclear NMR spectroscopy, single crystal X-ray diffraction and IR spectroscopy. The systematic nature of the approach of the synthesis and the high purity of the compounds enable a comparative investigation of the coordination behavior of pnictogenylboranes. The influences of the metal center, the pnictogen atom and the substituent at the pnictogen atom on the coordination behavior of pnictogenylboranes are compared.

## Introduction

Transition metal complexes bearing phosphine ligands have been of scientific interest for many years, and still are, due to their broad field of potential applications.[1] Important fields of application include antitumor therapies, enantioselective catalysis and luminescence compounds, as reported e.g. for copper-phosphine complexes.[2] Also, similar arsine complexes are of interest, even though the number of the reported compounds is much smaller, especially for primary arsines.[3] Being closely related to phosphines or arsines and also exhibiting an interesting reactivity due to their polar bond situation and additional reactive sites, group 13–15 compounds have been spotlighted by current research. E.g., for phosphine-boranes, mostly dehydrocoupling reactions were investigated.[4] Over the last decades, our group has contributed to this field by investigating the group 13–15 analogs to alkenes, stabilized only by a Lewis-base (LB), $R_2E{-}BH_2\cdot LB$ (E=P, As; R=H, Ph, *t*Bu, Figure 1)[5] and has reported their reactivity towards main group Lewis acids,[5e–g,6] their oxidation with chalcogenes[5a,e,7] and their use as building blocks for oligomeric and polymeric compounds.[5c,d,g,8] In contrast, their reactivity towards transition metal complexes was only investigated on a limited scale.

For the reaction of the parent phosphanylborane **Ia** towards the early transition metal complex $Cp_2Ti$(btmsa) (btmsa = bis(trimethylsilyl)acetylene), adduct formation at low temperature as well as at room temperature by using several equivalents of **Ia** the formation of coordination oligomers incorporating multiple metal centers was observed.[9] For late transition metal complexes, the coordination towards $Cu^I$ centers was reported for the parent compound **Ia**[10] as well as for the diphenyl-substituted derivative **IIIa**.[11] In a similar manner, the reaction of **IIIa** with $Ag^I$ salts has been investigated.[12] When reacting **Ia** and **Ib** with a $Pt^0$ complex, the reaction proceeds under oxidative addition of the E–H bond to the Pt center.[13] When reacting various pncitogenylboranes with (tht)AuCl, the resulting complexes reveal aurophilic interactions resulting in photoluminescent properties.[14]

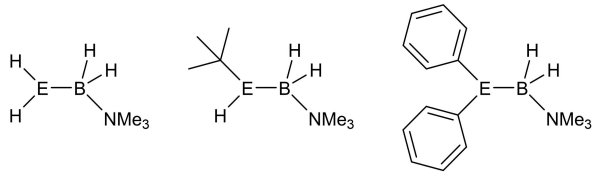

E = P: **Ia** E = As: **Ib** | E = P: **IIa** E = As: **IIb** | E = P: **IIIa** E = As: **IIIb**

**Figure 1.** Selected examples of pnictogenylboranes reported in recent years.

[a] *M.Sc. F. Lehnfeld, Dr. O. Hegen, Dr. G. Balázs, Prof. Dr. M. Scheer*
*Department of Inorganic Chemistry, University of Regensburg*
*93040 Regensburg (Germany)*
*E-mail: manfred.scheer@ur.de*
Homepage: https://www.uni-regensburg.de/chemie-pharmazie/anorganische-chemie-scheer/
[b] *Prof. A. Y. Timoshkin*
*Institute of Chemistry, St. Petersburg State University, Universitetskaya emb. 7/9, 199034 St. Petersburg (Russia)*

Supporting information for this article is available on the WWW under https://doi.org/10.1002/zaac.202200265

Special Collection *This article is part of a Special Collection dedicated to Professor Sjoerd Harder on the occasion of his 60th birthday. Please see our homepage for more articles in the collection.*

Considering the recently reported bidentate phosphanyl- and arsanylboranes[15] as well as the increasing interest in longer or mixed-element chain pnictogenylboranes,[16] a further investigation of the coordination behavior of pnictogenylboranes was the next step, especially focusing on the less frequently investigated earlier transition metals.

We report the coordination behavior of pnictogenylboranes towards group 6 complexes as transition metal Lewis acids. Their accessibility in good yields and high purity enables this system to serve as a model system for the coordination behavior of LB-stabilized pnictogenylboranes in general. The influence of the metal center, the pnictogen atom and the substituents on the pnictogen atom have been studied.

## Results and Discussion

The reaction of the Lewis acidic group 6 carbonyl complexes $[(CO)_4M(nbd)]$ (nbd = norbornadiene, M = Cr, Mo, W) with different LB-stabilized pnictogenylboranes of the type $RHEBH_2 \cdot NMe_3$ (E = P, As, R = H, *t*Bu) leads to the formation of the coordination compounds $[M(CO)_4(HREBH_2 \cdot NMe_3)_2]$ (Scheme 1). After addition of the pnictogenylborane to a toluene solution of the respective norbornadiene complex and stirring for 16 h at r.t., yellow to brown precipitate is formed, often already crystalline. In case of the arsenic derivatives **4**–**6**, a color change from yellow to brown becomes visible. The reactions proceed selectively and almost quantitively according to the $^{31}P$ and $^{11}B$ NMR spectroscopy of the crude reaction solutions. While being almost insoluble in non-polar solvents and exhibiting only moderate solubility in polar solvents, crystalline products can be isolated by layering of saturated $CH_2Cl_2$ solutions of the compounds **1**–**8** with *n*-hexane at r.t. or 6 °C and washing the crystalline solid with *n*-hexane. All compounds can be isolated in moderate to good crystalline yields, although the yields have not been optimized in terms of analytically pure precipitate.

All coordination compounds of $PH_2BH_2 \cdot NMe_3$ (**1**–**3**) reveal a broad singlet in the respective $^{31}P\{^1H\}$ NMR spectrum due to the coupling with the boron atom. In case of the tungsten compound **3**, a broadening of the signal with a half-height width of about 157 Hz occurs, to be the reason why no coupling with the tungsten nuclear can be observed. In all cases, a downfield shift of the $^{31}P$ signal compared to the starting material is observed. A clear trend in the shift can be noted from the W to the Cr complex with a shift for compound **3** at $\delta = -170.3$ ppm, for **2** at $\delta = -157.1$ ppm and for the chromium compound **1** at $\delta = -116.5$ ppm. In the $^{31}P\{^1H\}$ NMR spectra of all three compounds, further splittings are revealed. The P–H coupling constants are also dependent on the metal center, being smaller in the Cr compound **1** ($^1J_{P,H} = 265$ Hz), whereas the coordination products of the heavier homologs reveal a similar coupling constant of $^1J_{P,H} = 280$ Hz (**2** and **3**). However, in all cases, the coupling constants are approx. 80–90 Hz larger than in the starting material $PH_2BH_2 \cdot NMe_3$.

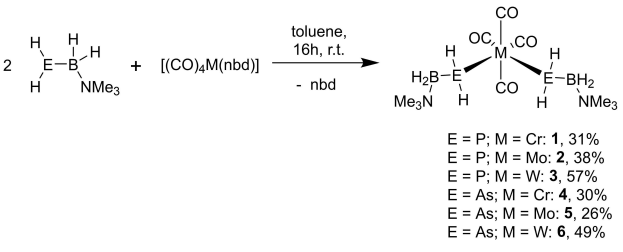


**Scheme 1.** General syntheses of group 6 coordination compounds (**1**–**6**) starting from parent pnictogenylboranes.

In the $^{11}B\{^1H\}$ NMR spectra, compounds **1** and **3** show broad multiplets, **2** only a broad singlet, all with very similar chemical shifts, exhibiting an upfield shift of about 1 ppm compared to $PH_2BH_2 \cdot NMe_3$. (**1**: $\delta = -7.72$ ppm; **2**: $\delta = -7.75$ ppm; **3**: $\delta = -7.52$ ppm). For **1** and **3**, $^1J_{P,B}$ coupling constants can be determined (**1**: 66 Hz; **3**: 64 Hz). In the $^{11}B$ NMR spectra of **2** and **3**, further splittings into broad triplets can be noticed (**2**: $^1J_{B,H} = 132$ Hz; **3**: $^1J_{B,H} = 130$ Hz), which for **1**, is only a very strong broadening of the signal.

In the $^1H$ NMR spectra of all three compounds **1**–**3**, the signals for the $PH_2$ moiety can be assigned to around $\delta = 2.7$ ppm. The signals corresponding to the $BH_2$ group can only be observed for **3** at $\delta = 2.34$ ppm. For the other two compounds, the signals show too much broadening but can be allotted to the range between 2 and 2.5 ppm.

The comparison of the different coordination compounds exhibits a clear trend, especially considering the chemical shifts and coupling constants of the phosphorus atoms in **1**–**3**, with the influence of the different metals on the respective data of the $BH_2$ moiety being minor. This trend matches the electronegativity and polarizability of the group 6 metals nicely, indicating more backbonding in the case of the heavier homologs. This is in accordance with phosphine complexes of group 6 metals in general.[17]

The molecular structure in the solid state of **1**–**3** has been determined by single crystal X-ray diffraction analysis (**1**: Figure 2; **2**–**3**: supporting information). All three compounds crystallize in the space group $P2_1/n$ and reveal a similar molecular structure. In all cases, the phosphanylborane molecules are located at the coordination site in *cis*-position on the $M(CO)_4$-fragment. Apart from the CO groups, all bonds are in the range of single bonds. The B–P bond adapts an antiperiplanar arrangement, whereas the $BH_2NMe_3$ moieties arrange in a trans position to the P–M–P plane. The P–M–P angles for all three compounds are below 90° (**1**: 86.83°; **2**: 85.68°; **3**: 85.44°) and therefore deviate slightly from the perfect octahedral structure, most likely due to steric effects.

Also, for the parent arsanylborane $AsH_2BH_2 \cdot NMe_3$, the substitution of norbornadiene proceeds in a selective manner. Compounds **4**–**6** have been characterized by multinuclear NMR spectroscopy. In the $^{11}B\{^1H\}$ NMR spectra, singlets at $\delta = -7.01$ ppm (**4**), $\delta = -7.24$ ppm (**5**) and $\delta = -7.36$ ppm (**6**), respectively, are observed. The $^{11}B$ NMR spectra of both compounds reveal additional splitting with similar coupling constants for all three complexes (**4**: $^1J_{B,H} = 115$ Hz; **5** and **6**: $^1J_{B,H} = 112$ Hz).

 

Journal of Inorganic and General Chemistry
ZAAC
Zeitschrift für anorganische und allgemeine Chemie





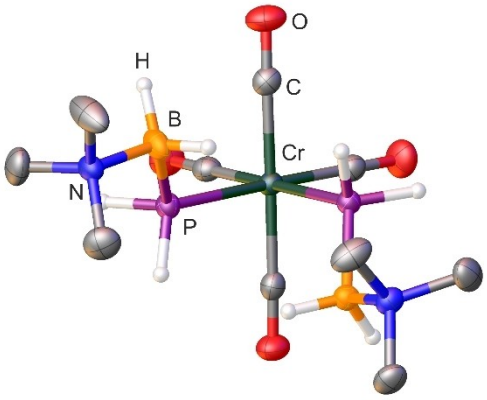


**Figure 2.** Molecular structure of **1**. Thermal ellipsoids are displayed at 50 % probability. Carbon-bound hydrogen atoms are omitted for clarity. Selected bond distances (Å) and angles [°]: Cr1–P1 2.3979(4), Cr1–P2 2.3998(4), P1–B1 1.9576(17), P2–B2 1.9565(18), N1–B1 1.612(2), N2–B2 1.613(2); P1–Cr1–P2 86.8(1), B1–P1–Cr1 119.0(1), B2–P2–Cr1 119.1(5), N2–B2–P2 115.6(1), N1–B1–P1 115.7(1).

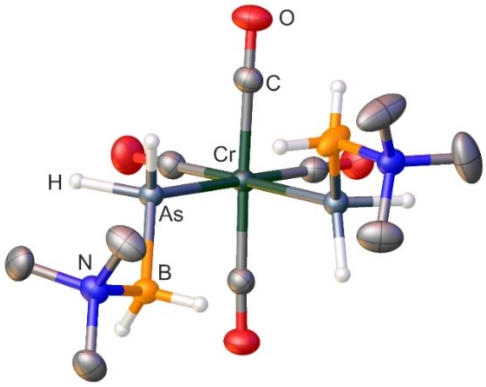


**Figure 3.** Molecular structure of **4**. Thermal ellipsoids are displayed at 50 % probability. Carbon-bound hydrogen atoms are omitted for clarity. Selected bond distances (Å) and angles [°]: As1–Cr1 2.4968(3), As1–B1 2.0670(19), As2–Cr1 2.4960(3), As2–B2 2.059(2), N1–B1 1.607(2), N2–B2 1.604(3); B1–As1–Cr1 119.70(6), B2–As2–Cr1 119.13(6), As2–Cr1–As1 86.066(10), N1–B1–As1 115.19(12), N2–B2–As2 116.04(14).

In the $^{1}$H NMR spectra, the expected broad multiplet corresponding to the $BH_2$ moiety is detected at approx. $\delta =$ 2.5 ppm and in both cases partly overlapped by the signal corresponding to the $NMe_3$ group at about $\delta = 2.8$ ppm. The $AsH_2$ groups reveal multiplets at $\delta = 1.15$ ppm (**4**), $\delta = 1.19$ ppm (**5**) and $\delta = 1.50$ ppm (**6**), respectively. A trend for a larger upfield shift in compounds **4** and **5** can be observed, which correlates with the less electropositive nature of tungsten compared to molybdenum and chromium. This trend is similar to the trend observed for the shifts of the phosphorus atoms in the $^{31}P\{^{1}H\}$ NMR spectra of **1**–**3**.

For **4**–**6**, crystals suitable for single crystal X-ray diffraction have been obtained, although for **5** only in poor crystalline yield. All three compounds crystallize in the space group $P2_1/n$ and reveal a similar molecular structure (**4**: Figure 3, **5**–**6**: supporting information). In all cases, the molecular structures are almost identical to the phosphorus analogs **1**–**3**. All observed bond lengths are in the range of single bonds, except for the CO bonds, which exhibit the expected bond lengths in the range of C–O multiple bonds. The bond angles reveal a similar trend for the As–M–As angle as observed for **1**–**3**, being slightly below 90° due to steric effects.

To investigate the influence of an organic substituent at the pnictogen atom, the reaction of $[(CO)_4M(nbd)]$ (M = Cr, W) with $t$BuPHBH$_2$·NMe$_3$ was performed (Scheme 2). In both cases, the products **7**–**8** are formed selectively and almost quantitively according to the $^{31}$P NMR spectroscopic investigation of the crude reaction mixture. **7** and **8** can be isolated as yellow blocks in moderate yields, which are lower compared to **1**–**3** due to an increased solubility. Both compounds were characterized by multinuclear NMR spectroscopy and single crystal X-ray diffraction.

The $^{31}P\{^{1}H\}$ NMR spectra of the two compounds reveal interesting differences compared to the unsubstituted analogs: In both cases, two signals can be observed at $\delta = -7.3$ ppm and

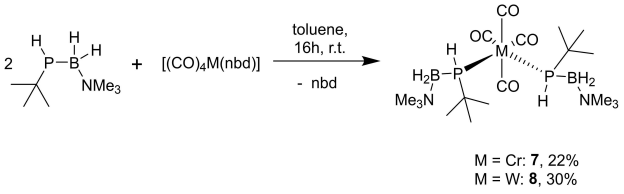


**Scheme 2.** Syntheses of group 6 coordination products of a substituted phosphanylborane (compounds **7**–**8**).

$\delta = -15.9$ ppm for **7** and at $\delta = -46.4$ ppm and $\delta = -50.7$ ppm for **8**, respectively. All signals appear as broad singlets due to the coupling with the boron atom, which in case of **8** results in no observable tungsten coupling (half-height width = 157 Hz). Due to the asymmetric nature of $t$BuPHBH$_2$NMe$_3$, two different diastereomers can be formed in these products, the *d/l* and the *meso* isomer, both of which appear in the $^{31}$P NMR spectra. In case of the 3d element Cr, the D/L isomer is favored due to the steric repulsion of the $t$Bu groups, which can be observed in a 5:1 ratio of the products according to the $^{31}P\{^{1}H\}$ NMR spectroscopy. For the heavier 5d metal tungsten, both signals appear in a 1:1 integral ratio, with no diastereomer being favored during the synthesis. In the $^{31}$P NMR spectra, all signals split into doublets, with similar $^{1}J_{P,H}$ coupling constants of ca. 260 Hz, which are comparable but slightly smaller than in compounds **1**–**3**. As compared to the starting material, for the complexes incorporating the parent phosphanylborane, a downfield shift is observed which is larger in the case of the chromium complex.

The $^{11}B\{^{1}H\}$ NMR spectra of **7** and **8** are similar to each other, revealing a broad singlet at $\delta = -4.7$ ppm, due to the overlap of the signals for the two isomers. Nevertheless, from the $^{31}$P NMR spectra, a similar $^{1}J_{P,B}$ of about 58 Hz can be identified for both compounds. In the $^{11}$B NMR spectra, the observed signals show

 

only broadening instead of further splitting due to the B–H coupling.

In the $^1$H NMR spectra, the signals corresponding to the P–H group (**7**: δ = 2.79 ppm; **8**: δ = 3.15 ppm) can be assigned. In both cases, the signals corresponding to the $BH_2$ group reveal broad signals in the range between 2 and 3 ppm. Due to the mixture of two diastereomers, the signals corresponding to the *t*Bu group appear slightly different: for **7**, a doublet at δ = 1.22 ppm ($^3J_{P,H}$ = 12 Hz) for the main product as well as a smaller doublet at δ = 1.27 ppm for the other isomer can be identified. In the case of **8**, the two doublets at δ = 1.25 ppm and δ = 1.21 ppm overlap forming a pseudo triplet due to the almost identical coupling constant ($^3J_{P,H}$ = 13 Hz). In the case of **8**, for both isomers, two almost identical singlets are observed at δ = 2.75 ppm and δ = 2.74 ppm, respectively, but unfortunately none can be assigned to one specific isomer.

The molecular structure in the solid state of **7** and **8** was determined by single crystal X-ray diffraction analysis (Figure 4). Again, due to the asymmetric nature of the starting material, there are some differences. Whereas **7**, crystallizing in the acentric space group $P2_1$, reveals both the D and L isomer in the unit cell, **8** only crystallizes as *meso*-isomer. This can be explained by the fact that the two bulky *t*Bu groups are able to occupy a *cis*-position relative to the P–W–P plane due to lower steric repulsion in the coordination sphere of the tungsten atom. Apart from these differences, the structures are relatively like the already discussed structures for **1**–**6** with all bond lengths and bond angles found in the expected ranges.

In addition to the X-ray diffraction analysis and the NMR spectroscopy, also mass spectrometry was applied for all compounds. ESI-MS of **1**, **2**, **4**, **5**, **7** and **8** in $CH_3CN$ reveals the respective molecular ion peak as well as multiple fragmentation peaks for decarbonylation products occurring during ionization. For **3** and **6**, LIFDI-MS has been performed, only revealing the molecular ion peaks.

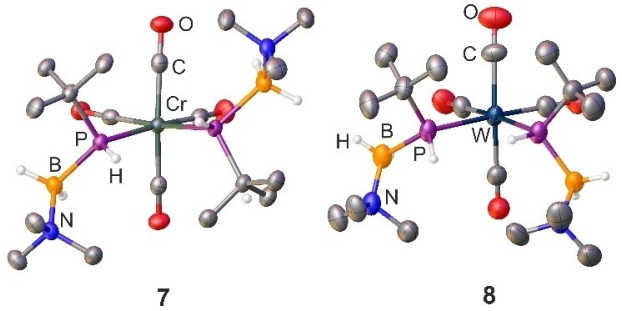


**Figure 4.** Molecular structure of **7** and **8**. Thermal ellipsoids are displayed at 50% probability. Carbon-bound hydrogen atoms are omitted for clarity. Selected bond distances (Å) and angles [°] for **7**: Cr1–P1 2.4336(8), Cr1–P2 2.4251(8), N1–B1 1.620(4), P1–C1 1.890(3), N2–B2 1.618(5), P1–B1 2.003(4), P2–C8 1.890(3), P2–B2 1.997(4); P2–Cr1–P1 91.20(3), B1–P1–Cr1 116.44(11), B2–P2–Cr1 114.36(11), N2–B2–P2 115.8(2), N1–B1–P1 116.2(2). Selected bond distances (Å) and angles [°] for **8**: W1–P1 2.579(3), W1–P2 2.576(3), N1–B1 1.618(16), N2–B2 1.626(16), P1–B1 1.980(13), P2–B2 1.993(14); P2–W1–P1 90.11(9), B1–P1–W1 115.7(4), B2–P2–W1 114.6(5), N1–B1–P1 116.2(8), N2–B2–P2 114.4(9).

Additionally, all compounds were investigated in a comparative infrared spectroscopy analysis to obtain further insight into the coordination behavior of the pnictogenylboranes. Selected stretching frequencies are summarized in Table 1.

The CO stretching frequencies of the compounds reveal several trends. All compounds share one common feature, showing significantly lower CO stretching frequencies than the respective starting materials [$(CO)_4$M(nbd)] (M = Cr, Mo, W), indicating the weaker π acceptor property of the pnictogenylboranes compared to the norbornadiene ligand. The most significant differences occur for the highest CO stretching band ($A_1$, axial CO), which mainly depends on the nature of the metal, all others are similar across all investigated compounds. Noticeably, there is a significant difference for the chromium complexes, with CO stretching frequencies by up to 15 $cm^{-1}$ smaller than the analogous molybdenum complexes.

Considering the donor/acceptor strength, a small but consistent difference between the arsanylborane and the phosphanylborane complexes are observed. However, the difference is small compared to the effect of the introduced *t*Bu group. The tungsten complex of the *t*Bu-substituted phosphanylborane **8** differs the most, pointing to having the strongest effect within the phosphanylboranes as ligands.

Computational studies (see SI for details) indicate that the stability of the [$M(CO)_4(HREBH_2 \cdot NMe_3)_2$] compounds slightly increase in order Cr < Mo < W, and decreases in order H > *t*Bu, which is due to steric bulk of *t*Bu substituents and is also consistent with the longer (by 0.027–0.034(1) Å) distances in **7** compared to **1**. Computed CO stretching frequencies shifts are consistent with experimental IR spectra.

## Conclusions

In summary, different pnictogenylboranes have been systematically coordinated towards group 6 transition metal Lewis acids. The obtained complexes incorporating phosphanylborane [$(CO)_4M(PH_2BH_2 \cdot NMe_3)_2$] (M = Cr, Mo, W; **1**–**3**), arsanylborane ([$(CO)_4M(AsH_2BH_2 \cdot NMe_3)_2$] (M = Cr, Mo, W; **4**–**6**) and *t*Bu-substituted phoshanylborane [$(CO)_4M(t$BuPHBH$_2 \cdot NMe_3)_2$] (M = Cr, W; **7**–**8**) have been fully characterized by multinuclear NMR

**Table 1.** Comparison of selected CO stretching frequencies of **1**–**6**, **8** and [$(CO)_4$M(nbd)][18] obtained by IR spectroscopy.

| Compound | $\nu_1$ [$cm^{-1}$] | $\nu_2$ [$cm^{-1}$] | $\nu_3$ [$cm^{-1}$] |
|---|---|---|---|
| **1** | 1993 | 1869 | 1822 |
| **2** | 2006 | 1876 | 1827 |
| **3** | 2002 | 1866 | 1820 |
| **4** | 1989 | 1865 | 1816 |
| **5** | 2004 | 1874 | 1820 |
| **6** | 1999 | 1862 | 1814 |
| **7** | 1977 | 1845 | 1818 |
| **8** | 1986 | 1854 | 1816 |
| [$(CO)_4$Cr(nbd)] | 2032 | 1980 | 1923 |
| [$(CO)_4$Mo(nbd)] | 2071 | 1980 | 1920 |
| [$(CO)_4$W(nbd)] | 2014 | 1939 | 1893 |

 

spectroscopy, single crystal X-ray diffraction, mass spectrometry and infrared spectroscopy. The good yields and high purity of the obtained compounds allowed their use as a model system to investigate the coordination behavior of pnictogenylboranes. It was possible to utilize the obtained analytical data to work out systematic trends within this family of compounds and therefore deepen the understanding of the coordination behavior of pnictogenylboranes towards early transition metals. In all cases, the resulting complexes show a similar solid-state structure but reveal significant differences according to multinuclear NMR spectroscopy and IR spectroscopy, most notably for the different metal centers. The effect on the coordination behavior of pnictogenylboranes possessing an organic substituent at the pnictogen atom in comparison to the parent compounds clearly dominates. An influence of the donating pnictogen atom could be observed but appeared to be rather small compared to the effect of the used (organic) substituent.

## Experimental Section

### General remarks

All reactions were performed under Argon or Nitrogen inert gas atmosphere using standard glovebox and Schlenk techniques. All solvents were taken from a solvent purification system of the type MB-SPS-800 of the company MBRAUN and degassed by standard procedures.

All NMR spectra were recorded on a Bruker Avance 400 spectrometer ($^{1}$H: 400.13 MHz, $^{13}$C{$^{1}$H}: 100.623 MHz, $^{11}$B: 128.387 MHz) with δ [ppm] referenced to external standards ($^{1}$H and $^{13}$C{$^{1}$H}: $SiMe_4$, $^{11}$B: $BF_3$–$Et_2O$). The C, H, N analyses were measured on an Elementar Vario EL III apparatus. All ESI-MS measurements were performed on a Micromass LCT ESI-TOF, all LIFDI-MS measurements on a Jeol AccuTOF GCX spectrometer. IR spectra were recorded as solids using a ThermoFisher Nicolet iS5 FT-IR spectrometer with an iD7 ATR module and an ITX Diamond crystal.

### Synthesis of $[(CO)_4Cr(PH_2BH_2\cdot NMe_3)_2]$ (1)

To a solution of $[(CO)_4Cr(nbd)]$ (nbd = norbornadiene, 0.25 mmol, 65 mg) in 2 mL toluene, a solution of $PH_2BH_2\cdot NMe_3$ (0.5 mmol, 53 mg) in 1 mL toluene is added at r.t. After stirring for 16 h at r.t., the solvent is removed *in vacuo*. The remaining yellow solid is washed three times with 2 mL *n*-hexane. By layering a saturated $CH_2Cl_2$ solution with *n*-hexane at 279 K, compound **1** can be isolated as yellow blocks. Yield: 29 mg (0.078 mmol, 31 %); $^{1}$H-NMR ($C_6D_6$, 293 K) δ = 2.65 (4H, dm, $^{1}J_{P,H}$ = 270 Hz, $PH_2$), 2.6–1.8 (4H, br, $BH_2$), 1.76 (18H, s, $NMe_3$). $^{31}$P NMR ($C_6D_6$, 293 K) δ = −116.5 (t, $^{1}J_{P,H}$ = 265 Hz, $PH_2$). $^{31}$P{$^{1}$H} NMR ($C_6D_6$, 293 K) δ = −116.5 (s (br), $PH_2$). $^{11}$B NMR ($C_6D_6$, 293 K) δ = −7.7 (br, $BH_2$). $^{11}$B{$^{1}$H} NMR ($C_6D_6$, 293 K) δ = −7.7 (br, $BH_2$). IR: $\tilde{\nu}$ = 3008 vw, 2948 vw, 2393 w, 2373 w, 2304 w, 1992 m, 1869 s, 1822 s, 1481 m, 1461 m, 1406 vw, 1243 w, 1150 m, 1123 m, 1095 m, 1060 w, 1011 w, 978 vw, 853 w, 796 m, 784 m, 688 s, 671 s, 657 s, 623 m; ESI-MS ($CH_3CN$) *m/z*: 374.12 ($M^+$), 346.13 ($M^+$–CO).

### Synthesis of $[(CO)_4Mo(PH_2BH_2\cdot NMe_3)_2]$ (2)

To a solution of $[(CO)_4Mo(nbd)]$ (nbd = norbornadiene, 0.25 mmol, 75 mg) in 2 mL toluene, a solution of $PH_2BH_2\cdot NMe_3$ (0.5 mmol, 53 mg) in 1 mL toluene is added at r.t. After stirring for 16 h at r.t., the solvent is removed *in vacuo*. The remaining yellow solid is washed three times with 2 mL *n*-hexane. By layering a saturated $CH_2Cl_2$ solution with *n*-hexane at 279 K, compound **2** can be isolated as yellow blocks. Yield: 45 mg (0.095 mmol, 38 %); $^{1}$H-NMR ($CD_2Cl_2$, 293 K) δ = 2.73 (18H, s, $NMe_3$), 2.6–1.8 (4H, br, $BH_2$), 2.45 (4H, dm, $^{1}J_{P,H}$ = 276 Hz, $PH_2$). $^{31}$P NMR ($CD_2Cl_2$, 293 K) δ = −157.2 (t, $^{1}J_{P,H}$ = 278 Hz, $PH_2$). $^{31}$P{$^{1}$H} NMR ($CD_2Cl_2$, 293 K) δ = −157.2 (s (br), $PH_2$). $^{11}$B NMR ($CD_2Cl_2$, 293 K) δ = −7.7 (t(br), $^{1}J_{B,H}$ = 132 Hz, $BH_2$). $^{11}$B{$^{1}$H} NMR ($CD_2Cl_2$, 293 K) δ = −7.7 (br, $BH_2$). IR: $\tilde{\nu}$ = 3006 vw, 2948 vw, 2392 w, 2371 w, 2309 w, 2006 m, 1876 s, 1827 s, 1481 m, 1461 m, 1405 vw, 1243 w, 1149 m, 1122 m, 1094 m, 1058 w, 1010 w, 977 vw, 851 w, 780 s, 769 s, 701 w, 648 s, 637 s, 623 m, 611 m; ESI-MS ($CH_3CN$) *m/z*: 418.07 ($M^+$), 389.07 ($M^+$–CO), 360.06 ($M^+$–2CO), 333.06 ($M^+$–3CO).

### Synthesis of $[(CO)_4W(PH_2BH_2\cdot NMe_3)_2]$ (3)

To a solution of $[(CO)_4W(nbd)]$ (nbd = norbornadiene, 0.25 mmol, 99 mg) in 2 mL toluene, a solution of $PH_2BH_2\cdot NMe_3$ (0.5 mmol, 53 mg) in 1 mL toluene is added at r.t. After stirring for 16 h at r.t., the solvent is removed *in vacuo*. The remaining yellow solid is washed three times with 2 mL *n*-hexane. By storing a saturated $CH_2Cl_2$ solution at 245 K, compound **3** can be isolated as yellow blocks. Yield: 72 mg (0.143 mmol, 57 %); $^{1}$H-NMR ($CDCl_3$, 293 K) δ = 2.82 (4H, dm, $^{1}J_{P,H}$ = 280 Hz, $PH_2$), 2.76 (18H, s, $NMe_3$), 2.34 (4H, m, $^{1}J_{B,H}$ = 130 Hz, $BH_2$). $^{31}$P NMR ($CDCl_3$, 293 K) δ = −170.3 (t, $^{1}J_{P,H}$ = 278 Hz, $PH_2$). $^{31}$P{$^{1}$H} NMR ($CDCl_3$, 293 K) δ = −170.3 (m, $^{1}J_{P,B}$ = 64 Hz, hhw = 157 Hz, $PH_2$). $^{11}$B NMR ($CDCl_3$, 293 K) δ = −7.5 (t(br), $^{1}J_{B,H}$ = 130 Hz, $BH_2$). $^{11}$B{$^{1}$H} NMR ($CDCl_3$, 293 K) δ = −7.5 (br, $^{1}J_{P,B}$ = 64 Hz, $BH_2$). IR: $\tilde{\nu}$ = 3003 vw, 2948 vw, 2394 w, 2373 w, 2310 w, 2002 m, 1866 s, 1820 s, 1480 m, 1461 m, 1405 vw, 1243 w, 1149 m, 1122 m, 1093 m, 1058 w, 1010 vw, 977 vw, 853 m, 788 s, 777 s, 704 m, 639 w, 624 vw; EA: calculated for $C_{10}H_{26}B_2N_2O_4WP_2$: C: 23.75 %; H: 5.18 %; N: 5.54 %; found: C: 23.99 %; H: 5.13 %; N: 5.43 %; LIFDI-MS ($CH_2Cl_2$) *m/z*: 504 ($M^+$).

### Synthesis of $[(CO)_4Cr(AsH_2BH_2\cdot NMe_3)_2]$ (4)

To a solution of $[(CO)_4Cr(nbd)]$ (nbd = norbornadiene, 0.25 mmol, 65 mg) in 2 mL toluene, a solution of $AsH_2BH_2\cdot NMe_3$ (0.5 mmol, 74 mg) in 1 mL toluene is added at r.t. After stirring for 16 h at r.t., the solvent is removed *in vacuo*. The remaining brown solid is washed three times with 2 mL *n*-hexane. By layering a saturated $CH_2Cl_2$ solution with *n*-hexane at 279 K compound **4** can be isolated as dark yellow blocks. Yield: 35 mg (0.075 mmol, 30 %); $^{1}$H-NMR ($CD_2Cl_2$, 293 K) δ = 2.78 (18H, s, $NMe_3$), 2.9–1.9 (4H, m, $^{1}J_{B,H}$ = 112 Hz, $BH_2$), 1.15 (4H, m, $AsH_2$). $^{11}$B NMR ($CD_2Cl_2$, 293 K) δ = −7.0 (t, $^{1}J_{B,H}$ = 112 Hz, $BH_2$). $^{11}$B{$^{1}$H} NMR ($CD_2Cl_2$, 293 K) δ = −7.0 (s, $BH_2$). IR: $\tilde{\nu}$ = 3007 vw, 2947 vw, 2414 w, 2382 w, 2112 w, 1989 m, 1865 s, 1816 s, 1480 m, 1460 m, 1406 vw, 1241 w, 1150 m, 1116 m, 1066 m, 1007 w, 979 w, 852 m, 723 m, 681 s, 644 s; EA: calculated for $C_{18}H_{42}B_2N_2O_4CrP_2$ : C: 26.01 %; H: 5.68 %; N: 6.07 %; found: C: 25.94 %; H: 5.45 %; N: 5.88 %.

### Synthesis of $[(CO)_4Mo(AsH_2BH_2\cdot NMe_3)_2]$ (5)

To a solution of $[(CO)_4Mo(nbd)]$ (nbd = norbornadiene, 0.25 mmol, 75 mg) in 2 mL toluene, a solution of $AsH_2BH_2\cdot NMe_3$ (0.5 mmol, 74 mg) in 1 mL toluene is added at r.t. After stirring for 16 h at r.t., the solvent is removed *in vacuo*. The remaining brown solid is

 

washed three times with 2 mL *n*-hexane. By layering a saturated $CH_2Cl_2$ solution with *n*-hexane at 279 K compound **5** can be isolated as dark yellow blocks. Yield: 33 mg (0.065 mmol, 26%); $^1$H-NMR ($CDCl_3$, 293 K) δ = 2.79 (18H, s, $NMe_3$), 2.9–1.9 (4H, m, $^1J_{B,H}$ = 112 Hz, $BH_2$), 1.19 (4H, m, $AsH_2$). $^{11}$B NMR ($CDCl_3$, 293 K) δ = −7.3 (t, $^1J_{B,H}$ = 112 Hz, $BH_2$). $^{11}$B{$^1$H} NMR ($CDCl_3$, 293 K) δ = −7.3 (s, $BH_2$). IR: $\tilde{\nu}$ = 3006 vw, 2947 vw, 2413 w, 2381 w, 2115 w, 2004 m, 1874 s, 1820 s, 1480 m, 1460 m, 1449 vw, 1405 vw, 1241 w, 1150 m, 1116 m, 1066 m, 1007 w, 978 w, 958 vw, 851 m, 718 m, 676 m, 629 w; ESI-MS ($CH_3CN$) *m/z*: 462.20 ($M^+$), 434.18 ($M^+$–CO); 405.20 ($M^+$–2CO).

### *Synthesis of [(CO)$_4$W(AsH$_2$BH$_2$·NMe$_3$)$_2$] (6)*

To a solution of [$(CO)_4$W(nbd)] (nbd = norbornadiene, 0.5 mmol, 196 mg) in 20 mL toluene, a solution of $AsH_2BH_2{\cdot}NMe_3$ (1 mmol, 149 mg) in 1 mL toluene is added at r.t. After stirring for 16 h at r.t., the solvent is removed *in vacuo*. The remaining brown solid is washed with 20 mL *n*-hexane. By storing a saturated $CH_2Cl_2$ solution at 245 K compound **6** can be isolated as yellow needles. Yield: 72 mg (0.245 mmol, 49%); $^1$H-NMR ($CDCl_3$, 293 K) δ = 2.81 (18H, s, $NMe_3$), 2.51 (4H, m, $^1J_{B,H}$ = 112 Hz, $BH_2$), 1.51 (4H, m, $AsH_2$). $^{11}$B NMR ($CDCl_3$, 293 K) δ = −7.4 (t, $^1J_{B,H}$ = 112 Hz, $BH_2$). $^{11}$B{$^1$H} NMR ($CDCl_3$, 293 K) δ = −7.4 (s, $BH_2$). IR: $\tilde{\nu}$ = 3006 vw, 2947 vw, 2415 w, 2383 w, 2117 w, 1999 m, 1862 s, 1814 s, 1480 m, 1459 m, 1405 vw, 1241 w, 1150 w, 1116 m, 1065 m, 1006 m, 978 w, 959 vw, 720 m, 678 s, 623 w; EA: calculated for $C_{10}H_{26}As_2N_2O_4WB_2$ : C: 20.23%; H: 4.41%; N: 4.71%; found: C: 20.52%; H: 4.49%; N: 4.54%; LIFDI-MS ($CH_2Cl_2$) *m/z*: 592 ($M^+$).

### *Synthesis of [(CO)$_4$Cr(tBuPHBH$_2$·NMe$_3$)$_2$] (7)*

[$(CO)_4$Cr(nbd)] (nbd = norbornadiene, 0.2 mmol, 51 mg) and *t*BuPHBH$_2$·NMe$_3$ (0.4 mmol, 64 mg) are dissolved in 4 mL toluene at r.t. After stirring for 16 h at r.t., the solvent is removed *in vacuo*. The remaining yellow solid is washed three times with 2 mL *n*-hexane. By layering a saturated $CH_2Cl_2$ solution with *n*-hexane at 293 K compound **7** can be isolated as yellow needles. Yield: 18 mg (0.040 mmol, 22%); $^1$H-NMR ($CD_2Cl_2$, 293 K) δ = 2.79 (2H, dm, $^1J_{P,H}$ = 266 Hz, PH), 2.74 (18H, s, $NMe_3$), 2.8–1.9 (4H, br, $BH_2$), 1.22 (18H, m, *t*Bu). $^{31}$P NMR ($CD_2Cl_2$, 293 K) δ = −7.3 (d, $^1J_{P,H}$ = 266 Hz, $PH_2$, *D/L*-isomer), −15.8 (d, $^1J_{P,H}$ = 266 Hz, $PH_2$, *meso*-isomer). $^{31}$P{$^1$H} NMR ($CD_2Cl_2$, 293 K) δ = −7.3 (s, $PH_2$, *D/L*-isomer), −15.8 (s, $PH_2$, *meso*-isomer). $^{11}$B NMR ($CD_2Cl_2$, 293 K) δ = −4.9 (br, $BH_2$). $^{11}$B{$^1$H} NMR ($CD_2Cl_2$, 293 K) δ = −4.9 (br, $BH_2$); ESI-MS ($CH_3CN$) *m/z*: 486 ($M^+$), 458 ($M^+$–CO); IR: $\tilde{\nu}$ = 2940 w, 2860 vw, 2397 w, 2266 w, 1977 m, 1845 s, 1818 s, 1485 m, 1460 m, 1406 vw, 1386 w, 1359 w, 1251 vw, 1164 w, 1127 m, 1083 m, 1018 w, 979 w, 934 vw, 841 m, 816 w, 780 w, 681 s, 647 s.

### *Synthesis of [(CO)$_4$W(tBuPHBH$_2$·NMe$_3$)$_2$] (8)*

[$(CO)_4$W(nbd)] (nbd = norbornadiene, 0.2 mmol, 78 mg) and *t*BuPHBH$_2$·NMe$_3$ (0.4 mmol, 64 mg) are dissolved in 4 mL toluene at r.t. After stirring for 16 h at r.t., the solvent is removed *in vacuo*. The remaining yellow solid is washed three times with 2 mL *n*-hexane. By layering a saturated $CH_2Cl_2$ solution with *n*-hexane at 293 K compound **8** can be isolated as yellow blocks. Yield: 33 mg (0.059 mmol, 30%); $^1$H-NMR ($CD_2Cl_2$, 293 K) δ = 3.16 (2H, dm, $^1J_{P,H}$ = 266 Hz, PH), 2.75 (9H, s, $NMe_3$), 2.75 (9H, s $NMe_3$), 2.8–1.9 (4H, br, $BH_2$), 1.21 (9H, d, *t*Bu). $^{31}$P NMR ($CD_2Cl_2$, 293 K) δ = −46.3 (d, $^1J_{P,H}$ = 266 Hz, hhw = 157 Hz, $PH_2$, *D/L*-isomer), −50.7 (d, $^1J_{P,H}$ = 266 Hz, $PH_2$, *meso*-isomer), $^{31}$P{$^1$H} NMR ($CD_2Cl_2$, 293 K) δ = −46.3 (s, $PH_2$, hhw = 157 Hz, *D/L*-isomer), −50.7 (s, $PH_2$, *meso*-isomer). $^{11}$B NMR ($CD_2Cl_2$, 293 K) δ = −4.8 (br, $BH_2$). $^{11}$B{$^1$H} NMR ($CD_2Cl_2$, 293 K) δ = −4.8 (br, $BH_2$); IR: $\tilde{\nu}$ = 2948 w, 2861 vw, 2397 w, 2270 w, 1986 w, 1854 m, 1816 vs, 1484 m, 1460 m, 1406 vw, 1359 w, 1253 m, 1188 m, 1126 m, 1081 w, 1020 w, 990 w, 860 m, 842 m, 817 w, 786 m, 696 vw, 609 m; EA: calculated for $C_{18}H_{42}B_2N_2O_4WP_2$ : C: 34.99%; H: 6.85%; N: 4.53%; found: C: 34.90%; H: 6.63%; N: 4.49%; ESI-MS ($CH_3CN$) *m/z*: 618 ($M^+$), 590 ($M^+$–CO).

### *Crystallographic details*

To characterize the products using single crystal X-ray diffraction, a small number of crystals were transferred into dried mineral oil. Thereafter, a suitable crystal was selected and mounted on a Rigaku SuperNova diffractometer with an Atlas detector (**3** and **6**), on a XTaLab Synergy R, DW system with Hy-Pix Arc detector (**7**–**8**) or a GV1000 with a TitanS2 detector (**1**–**2**, **4**–**5**) using MiTeGen loops. All data were collected at 123 K. The software CrysAlisPro (Version 41_64.93a) was used for data collection and data reduction.[19] For structure solution, ShelXT[20] was used and the subsequent data refinement was carried out with ShelXL.[21] Olex2[22] was taken for visualization. All atoms are depicted as ellipsoids with a 50% probability level.

Deposition numbers (2178104 for **1**), (2178105 for **2**), (2178106 for **3**), (2178107 for **4**), (2178108 for **5**), (2178109 for **6**), (2178110 for **7**) and (2178111 for **8**) contain the supplementary crystallographic data for this paper. These data are provided free of charge by the joint Cambridge Crystallographic Data Centre and Fachinformationszentrum Karlsruhe Access Structures service www.ccdc.cam.ac.uk/structures.

## Acknowledgements

This work was supported by the Deutsche Forschungsgemeinschaft (DFG) within the project Sche 384/41-1 and Russian Science Foundation (RSF project 21-43-04404). Use of computational resources of the Research center «Computing Center» of the research park of St. Petersburg State University is acknowledged. Open Access funding enabled and organized by Projekt DEAL.

## Conflict of Interest

The authors declare no conflict of interest.

## Data Availability Statement

The data that support the findings of this study are available in the supplementary material of this article.

**Keywords:** boron · coordination · group 13/15 compounds · pnictogen · transition metal

[1] a) A. Gallen, A. Riera, X. Verdaguer, A. Grabulosa, *Catal. Sci. Technol.* **2019**, *9*, 5504–5561; b) J. T. Fleming, L. J. Higham, *Coord. Chem. Rev.* **2015**, *297–298*, 127–145; c) I. V. Kourkine, S. V. Maslennikov, R. Ditchfield, D. S. Glueck, G. P. A. Yap, L. M. Liable-Sands, A. L. Rheingold, *Inorg. Chem.* **1996**, *35*, 6708–

 

6716; d) P. G. Edwards, B. M. Kariuki, P. D. Newman, H. A. Tallis, C. Williams, *Dalton Trans.* **2014**, *43*, 15532–15545.

[2] a) K. Tsuge, Y. Chishina, H. Hashiguchi, Y. Sasaki, M. Kato, S. Ishizaka, N. Kitamura, *Coord. Chem. Rev.* **2016**, *306*, 636–651; b) R. Czerwieniec, M. J. Leitl, H. H. H. Homeier, H. Yersin, *Coord. Chem. Rev.* **2016**, *325*, 2–28; c) V. W.-W. Yam, V. K.-M. Au, S. Y.-L. Leung, *Chem. Rev.* **2015**, *115*, 7589–7728; d) C. Marzano, F. Tisato, M. Porchia, M. Pellei, V. Gandin, in: *Copper(I) Chemistry of Phosphines, Functionalized Phosphines and Phosphorus Heterocycles* (Ed.: M. S. Balakrishna), Elsevier, **2019**, pp. 83–107; e) R. Narayan, in: *Copper(I) Chemistry of Phosphines, Functionalized Phosphines and Phosphorus Heterocycles* (Ed.: M. S. Balakrishna), Elsevier, **2019**, pp. 259–313; f) S. Evariste, A. M. Khalil, M. E. Moussa, A. K.-W. Chan, E. Y.-H. Hong, H.-L. Wong, B. Le Guennic, G. Calvez, K. Costuas, V. W.-W. Yam, C. Lescop, *J. Am. Chem. Soc.* **2018**, *140*, 12521–12526.

[3] a) O. M. A. Salah, M. I. Bruce, P. J. Lohmeyer, C. L. Raston, B. W. Skelton, A. H. White, *Dalton Trans.* **1981**, 962–967; b) G. A. Bowmaker, E. Effendy, R. D. Hart, J. D. Kildea, A. H. White, *Aust. J. Chem.* **1997**, *50*, 653–670; c) M. F. Davis, M. Jura, W. Levason, G. Reid, M. Webster, *J. Organomet. Chem.* **2007**, *692*, 5589–5597; d) J. R. Black, W. Levason, M. D. Spicer, M. Webster, *Dalton Trans.* **1993**, 3129–3136.

[4] a) H. C. Johnson, A. S. Weller, *Angew. Chem. Int. Ed.* **2015**, *54*, 10173–10177; *Angew. Chem.* **2015**, *127*, 10311–10315; b) H. C. Johnson, E. M. Leitao, G. R. Whittell, I. Manners, G. C. Lloyd-Jones, A. S. Weller, *J. Am. Chem. Soc.* **2014**, *136*, 9078–9093; c) A. N. Marziale, A. Friedrich, I. Klopsch, M. Drees, V. R. Celinski, J. Schmedt auf der Günne, S. Schneider, *J. Am. Chem. Soc.* **2013**, *135*, 13342–13355; d) S. Pandey, P. Lönnecke, E. Hey-Hawkins, *Eur. J. Inorg. Chem.* **2014**, *2014*, 2456–2465; e) D. Han, F. Anke, M. Trose, T. Beweries, *Coord. Chem. Rev.* **2019**, *380*, 260–286; f) J. A. Bailey, P. G. Pringle, *Coord. Chem. Rev.* **2015**, *297–298*, 77–90; g) R. T. Paine, H. Noeth, *Chem. Rev.* **1995**, *95*, 343–379.

[5] a) K.-C. Schwan, A. Y. Timoskin, M. Zabel, M. Scheer, *Chem. Eur. J.* **2006**, *12*, 4900–4908; b) U. Vogel, P. Hoemensch, K.-C. Schwan, A. Y. Timoshkin, M. Scheer, *Chem. Eur. J.* **2003**, *9*, 515–519; c) C. Marquardt, T. Jurca, K.-C. Schwan, A. Stauber, A. V. Virovets, G. R. Whittell, I. Manners, M. Scheer, *Angew. Chem. Int. Ed.* **2015**, *54*, 13782–13786; *Angew. Chem.* **2015**, *127*, 13986–13991; d) A. Stauber, T. Jurca, C. Marquardt, M. Fleischmann, M. Seidl, G. R. Whittell, I. Manners, M. Scheer, *Eur. J. Inorg. Chem.* **2016**, 2684–2687; e) O. Hegen, A. V. Virovets, A. Y. Timoshkin, M. Scheer, *Chem. Eur. J.* **2018**, *24*, 16521–16525; f) C. Marquardt, A. Adolf, A. Stauber, M. Bodensteiner, A. V. Virovets, A. Y. Timoshkin, M. Scheer, *Chem. Eur. J.* **2013**, *19*, 11887–11891; g) F. Lehnfeld, M. Seidl, A. Y. Timoshkin, M. Scheer, *Eur. J. Inorg. Chem.* **2022**, *2022*, e202100930.

[6] C. Marquardt, T. Kahoun, J. Baumann, A. Y. Timoshkin, M. Scheer, *Z. Anorg. Allg. Chem.* **2017**, *643*, 1326–1330.

[7] C. Marquardt, O. Hegen, T. Kahoun, M. Scheer, *Chem. Eur. J.* **2017**, *23*, 4397–4404.

[8] a) C. Marquardt, T. Kahoun, A. Stauber, G. Balázs, M. Bodensteiner, A. Y. Timoshkin, M. Scheer, *Angew. Chem. Int. Ed.* **2016**, *55*, 14828–14832; *Angew. Chem.* **2016**, *128*, 15048–15052; b) C. Marquardt, G. Balázs, J. Baumann, A. V. Virovets, M. Scheer, *Chem. Eur. J.* **2017**, *23*, 11423–11429; c) C. Marquardt, C. Thoms, A. Stauber, G. Balázs, M. Bodensteiner, M. Scheer, *Angew. Chem. Int. Ed.* **2014**, *53*, 3727–3730; *Angew. Chem.* **2014**, *126*, 3801–3804.

[9] C. Thoms, C. Marquardt, A. Y. Timoshkin, M. Bodensteiner, M. Scheer, *Angew. Chem. Int. Ed.* **2013**, *52*, 5150–5154; *Angew. Chem.* **2013**, *125*, 5254–5259.

[10] K.-C. Schwan, A. Adolf, M. Bodensteiner, M. Zabel, M. Scheer, *Z. Anorg. Allg. Chem.* **2008**, *634*, 1383–1387.

[11] M. Elsayed Moussa, J. Braese, C. Marquardt, M. Seidl, M. Scheer, *Eur. J. Inorg. Chem.* **2020**, *2020*, 2501–2505.

[12] M. Elsayed Moussa, C. Marquardt, O. Hegen, M. Seidl, M. Scheer, *New J. Chem.* **2021**, *45*, 14916–14919.

[13] U. Vogel, K.-C. Schwan, P. Hoemensch, M. Scheer, *Eur. J. Inorg. Chem.* **2005**, *2005*, 1453–1458.

[14] J. Braese, A. Schinabeck, M. Bodensteiner, H. Yersin, A. Y. Timoshkin, M. Scheer, *Chem. Eur. J.* **2018**, *24*, 10073–10077.

[15] O. Hegen, J. Braese, A. Y. Timoshkin, M. Scheer, *Chem. Eur. J.* **2019**, *25*, 485–489.

[16] O. Hegen, C. Marquardt, A. Y. Timoshkin, M. Scheer, *Angew. Chem. Int. Ed.* **2017**, *56*, 12783–12787; *Angew. Chem.* **2017**, *129*, 12959–12963.

[17] a) W.-L. Su, H.-P. Huang, W.-T. Chen, W.-Y. Hsu, H.-Y. Chang, S.-Y. Ho, S.-P. Wang, S.-G. Shyu, *J. Chin. Chem. Soc.* **2011**, *58*, 163–173; b) T. J. Malosh, S. R. Wilson, J. R. Shapley, *Inorg. Chim. Acta* **2009**, *362*, 2849–2855.

[18] E. Subasi, S. Karahan, A. Ercag, *Russ. J. Coord. Chem.* **2007**, *33*, 886–890.

[19] CrysAlisPro Software System, Rigaku Oxford Diffraction, **2020**.

[20] G. Sheldrick, *Acta Crystallogr. Sect. A* **2015**, *71*, 3–8.

[21] G. Sheldrick, *Acta Crystallogr. Sect. C* **2015**, *71*, 3–8

[22] O. V. Dolomanov, L. J. Bourhis, R. J. Gildea, J. A. K. Howard, H. Puschmann, *J. Appl. Crystallogr.* **2009**, *42*, 339–341.

Manuscript received: August 2, 2022
Revised manuscript received: August 19, 2022
Accepted manuscript online: August 22, 2022

 